The Astronomical Journal, 124:1746–1756, 2002 September

RADIAL VELOCITY STUDIES OF CLOSE BINARY STARS. VII. METHODS AND UNCERTAINTIES[1]

Slavek M. Rucinski
David Dunlap Observatory, University of Toronto, P.O. Box 360, Richmond Hill, ON L4C 4Y6, Canada; rucinski@astro.utoronto.ca
Received 2002 January 10; accepted 2002 June 13

ABSTRACT

Methods used in the radial velocity program of short-period binary systems at the David Dunlap Observatory are described with particular stress on the broadening-function formalism. This formalism makes it possible to determine radial velocities from the complex spectra of multiple-component systems with component stars showing very different degrees of rotational line broadening. The statistics of random errors of orbital parameters are discussed on the basis of the available orbital solutions presented in the six previous papers of the series, each with 10 orbits. The difficult matter of systematic uncertainties in orbital parameters is illustrated for the typical case of GM Dra from Paper VI.

Key words: binaries: close — binaries: eclipsing — stars: variables: other

1. INTRODUCTION

This paper should be considered a companion and supplement to the previous papers of our series of radial velocity studies of close binary stars: Lu & Rucinski (1999, Paper I); Rucinski & Lu (1999, Paper II); Rucinski, Lu, & Mochnacki (2000, Paper III); Lu, Rucinski, & Ogloza (2001, Paper IV); Rucinski et al. (2001, Paper V); Rucinski et al. (2002, Paper VI).

The current program of radial velocity observations of close binary systems with periods shorter than 1 day is approximately at its halfway point. Our methods have been evolving slightly during the execution of the 60 radial velocity orbits presented in the six papers of the series but appear to have stabilized now, warranting a more detailed documentation of the essential steps in our analysis and data reductions. We summarize these methods and give an overview of the uncertainties so that the results described in the previous and planned future papers of the series can be better evaluated by readers. The discussion is limited strictly to methodological aspects and does not include any astrophysical results, which will be discussed after the program is concluded.

2. INSTRUMENTATION AND OBSERVATIONS

We observe radial velocities of close binary stars with the 1.88 m telescope of the David Dunlap Observatory (DDO), using its medium-resolution spectrograph in the Cassegrain focus. The angular scale in the telescope focus is $6'' \text{ mm}^{-1}$. We use one of the two spectrograph slits, 300 or 250 μm in width, both fixed in the east-west orientation and both 10 mm long. The angular widths of $1''.8$ and $1''.5$ approximately match the median seeing at the DDO of $1''.7$. Since we started with the shortest-period binaries showing the strongest rotational line broadening, most observations have been made with the 300 μm slit. The scale reduction of the collimator-camera combination is 4 times, resulting in a slit image of 75 or 62 μm for either of the slits. Our light detector is currently a thick, front-illuminated CCD chip of 1024×1024 pixels, 19 μm square. Thus the slit images have the total widths of 3.9 or 3.3 pixels, while the FWHM widths are about 2.6 and 2.2 pixels for the respective slits. To lower the influence of the readout noise, the two-dimensional CCD images are on-chip binned four times in the direction perpendicular to the dispersion direction.

Most of the spectral data have been obtained using the 1800 line mm^{-1} diffraction grating, with the spectral window centered on the magnesium triplet Mg I *b* at 5184 Å. For solar-type stars this region is very rich in spectral lines, which is an essential consideration for our method of radial velocity measurements—through broadening functions—to succeed. The main-sequence stars of spectral types of middle-A to middle-K are practically the only stars found in close binaries with orbital periods shorter than one day. At 5184 Å the spectrograph delivers 0.204 Å/(19 μm pixel) or about 11.8 km s^{-1} pixel^{-1}. As is well known, when cross-correlation or similar techniques are used, narrow, properly sampled, symmetric spectral features can be usually measured to better than about 1/10 part of the pixel size, with the accuracy growing in relation to the total length of the spectrum. In our case the spectrum has the length of 208 Å so that we can rather easily determine velocities of sharp-line stars with an accuracy of about 1 km s^{-1}, as has been verified by many observational programs at the DDO (see the end of this section). The accuracy for broad-lined spectra of binary components is obviously lower and depends on a combination of many factors. We discuss the random errors in § 8, while systematic uncertainties specific to close binary stars are discussed in § 9.

The spectrograph is known to show some flexure limiting exposures to about 30 minutes. This has not been a real limitation in the observations, because our program stars have short periods and in fact require exposures to be no longer than 15–20 minutes to prevent the radial velocity smearing. We normally take comparison-lamp (FeAr) spectra before and after each exposure, but sometimes, for the shortest-period binaries, we take two or three stellar exposures for a set of bracketing comparison spectra spaced by no more than half an hour. The flat field lamp is an internal one in the spectrograph, but we occasionally take also sky flat-field spectra.

We observe typically three to five radial velocity standard stars per night. These stars are selected to have spectra of

[1] Based on data obtained at the David Dunlap Observatory, University of Toronto.

similar spectral types to our program stars, to serve later as templates in our technique of radial velocity measurements through broadening functions (see §§ 5–6). An intercomparison of radial velocities of standard stars gives an estimate of random errors at the level of about 1.0–1.2 km s^{-1}. This agrees with the results for Cepheids observed at the DDO by Sugars & Evans (1994) and Evans (2000), where the errors were estimated at 1.0–1.3 km s^{-1}. A fraction in these errors may come from our continuing use of the IAU standard-star list as published in the 1995 Nautical Almanac. As explained in Stefanik et al. (1999), at that time the IAU list contained a few stars that are unsuitable as radial velocity standards. Since we used many different standard stars from the IAU list, these systematic errors averaged out to some degree and manifested themselves mostly as random errors. We now use exclusively the list of Stefanik et al. (1999), but the results of our program may be affected by the uncertainties in the old standard velocity data at a level of 0.2–0.5 km s^{-1}.

3. INITIAL ANALYSIS OF SPECTRA

The reductions consist of several stages. Stage 1 consists of a transformation from two-dimensional images to one-dimensional, wavelength-calibrated, rectified spectra. All of the steps, starting with debiasing and flat-fielding, utilize the standard techniques within IRAF.[2] We make sure to use a consistent set of low-order polynomials for the dispersion relation and use the IRAF rejection algorithm for rectification of the spectra; both steps are facilitated by the short length of our spectra within which the dispersion and the CCD sensitivity vary only slightly and in a smooth way.

Figure 1 shows a typical spectrum for our program of the binary KR Com, one of the stars presented in the most recent paper of the series (Rucinski et al. 2002, Paper VI). It is a typical yet difficult case, in the sense that we frequently have been dealing with rather complex, multicomponent spectra, even among relatively bright stars (7th magnitude in this case). Some systems of our program have been previously known binaries, too difficult to handle using traditional (including cross-correlation) methods, but many were recently discovered as photometric variables.

The spectra of KR Com are dominated by the third, slowly rotating component which—although the fainter one in the visual system—dominates the spectral appearance and produces sharp, easily identifiable spectral lines. The

[2] IRAF is distributed by the National Optical Astronomy Observatory, which is operated by the Association of Universities for Research in Astronomy, Inc., under cooperative agreement with the National Science Foundation.

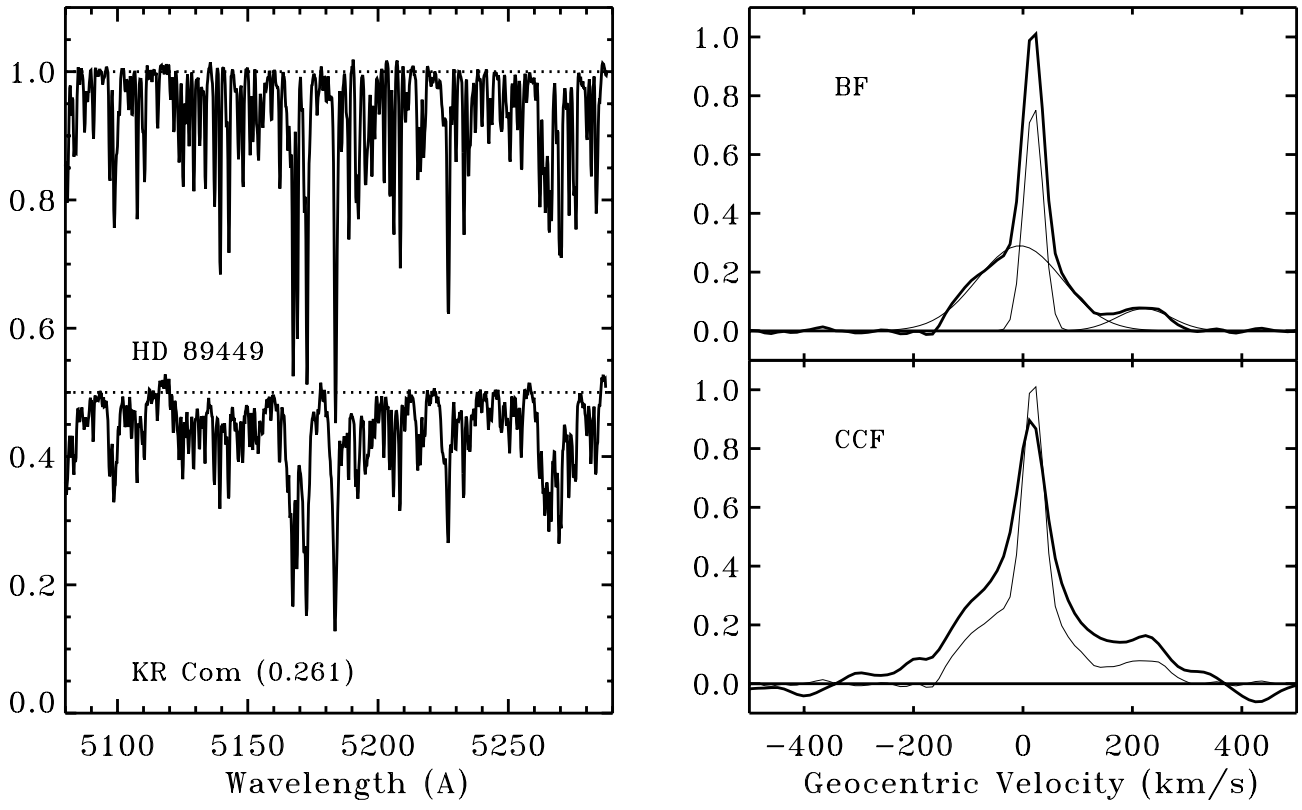

FIG. 1.—*Left*: Spectra of the sharp-line template star HD 89449 (*top spectrum*) and of the close binary star KR Com (*bottom spectrum*, shifted down by 0.5 in the observed flux). The spectral types of the stars are F6IV and G0IV, respectively. *Top right*: Broadening function (BF) obtained by our linear deconvolution using the two spectra in the left panel. When measuring radial velocities of a binary, we initially fit the whole triple feature by Gaussians then subtract the sharp-line component and repeat the determination for the close binary. The three components of the BF are shown by thin lines. *Bottom right*: Cross-correlation function (CCF, *thick line*), in comparison with the BF (*thin line*), both obtained from the same spectra at left. The CCF has much lower resolution than the BF, but also shows negative excursions in the zero (baseline) level. While Gaussians may be a reasonable tool for measurement of radial velocities from the CCFs, the BFs are much better defined; note the much steeper outer ends of the BF relative to the Gaussians. We discuss extensively the systematic uncertainties of this type in § 9.

triplicity of KR Com went apparently unnoticed for so long mostly because, superficially, the spectra look like those of a single, slowly rotating star and—paradoxically—the spectrum of the brighter binary component is not normally visible. The presence of the binary, which produces the broad spectral signature, manifests itself spectrally only through merging of more common, weaker lines and the general lowering of the continuum, and it is difficult to notice in low signal-to-noise ratio (S/N) spectra. The low-level photometric variability of the whole system is due to the contact binary, which is the brighter component in the system, but the variability signal is sufficiently "diluted" in the combined light of the system that it took the high quality of the *Hipparcos* photometry to discover it.

Spectra such as those shown in the left panel of Figure 1 are not analyzed directly but are subject to the broadening-function extraction process, which is followed by measurements of radial velocities.

4. WHY WE DO NOT USE THE CROSS-CORRELATION FUNCTION

Step 2 of the analysis is the determination of the broadening function (BF). The BF approach was described before in Rucinski (1992, 1999) and is discussed more extensively in § 5. In essence, it consists of a linear, least-squares determination of the broadening convolution kernel from rotationally—and orbitally—broadened spectra, utilizing spectra of sharp-line, slowly rotating radial velocity standards. We do not use the popular cross-correlation function (CCF) technique because it appears to give inferior and biased results for close binary systems. We now try to explain this rather strong statement.

1. The CCF *combines* the broadening of the program spectrum with that of the template, with a resulting loss of resolution, while the BF approach attempts to *remove* the common broadening contributions. Only if the template spectrum were a series of delta functions would the results be the same.
2. The definition of the baseline in the CCF is usually difficult and may lead to problems when relative luminosities of components are determined.
3. Outside of the main peak, which is used for radial velocity determination, the CCF always shows a fringing pattern, which may affect the strength and intensity of secondary correlation peaks for multiple systems. For very close binaries, the secondary fringes frequently produce the "peak-pulling" effect of the systematically smaller radial velocity amplitudes, but a more complex interaction is entirely possible.
4. The shape of the CCF beyond the main correlation peak depends on the shape of the stellar spectrum. *For the same star observations in different parts of the spectrum define different CCFs.* This problem is rarely recognized and is particularly severe for sparse spectra, when the CCF is analyzed over a wide range of correlation lags.

The problems listed above are illustrated in Figure 1 for the case of the triple system KR Com. In the right panel, we show a comparison of the BF with the CCF for the same spectra. While the BF very clearly shows all three components in the system, it would be very difficult separate the three signatures using the CCF. The superior resolution offered by the BF approach has permitted us to analyze spectra with very strong rotational broadening, combined with situations of three or more sets of blended lines in triple and quadruple systems, with component stars showing different amounts of rotational broadening. Such systems have frequently been abandoned in the past because of insurmountable difficulties with separating and measuring the radial velocities of individual components.

The problems of the baseline location and fringing in the CCF, as well as of the dependence on the shape of the stellar spectrum, are illustrated in Figure 2. This figure contains a result of the following data-processing experiment. A high-quality, but somewhat sparse, stellar spectrum (*left*, sampled at equal velocity steps of 0.88 km s^{-1}) was convolved with the single-star rotational-broadening pattern with $V \sin i = 88$ km s^{-1} and then subjected to the CCF determination. No noise was added, so the CCF is basically perfectly determined and can be used for a direct comparison with the assumed broadening function. The right panel of the figure compares the assumed broadening profile (*dotted line*), which is the same as the BF, with the CCF (*solid line*). The strong fringes in the CCF are very well visible. In this particular case, the unusual strength the positive fringes results from the low density of spectral features in the original spectrum and illustrates the dependence of the CCF on the stellar spectrum. While the BF formalism is insensitive to the density and distribution of the spectral lines, the CCF—beyond the main peak—does depend on the spectral region. Thus sparse spectra will lead to less well defined broadening functions with larger *random errors* (simply because of the lower information content), while the CCF will additionally show *systematic differences* in the fringing pattern outside the main peak.

The negative fringes that are always present in the CCF can produce a quasi baseline around the main correlation peak at a very different level than expected. In the case shown in Figure 2, the local baseline is located about −0.1 below the originally assumed broadening profile. If only a small part of the CCF were used, this is where the baseline would normally be located. Since a CCF would rarely be used for anything else but a radial velocity determination from the correlation peak, the exact location of the baseline may seem immaterial. However, when a secondary star is added to the picture, with the similar rotational broadening and a velocity separation comparable to the rotational broadening, as is the case for short-period binary stars, then the secondary peak in the CCF will definitely interact with the primary-star fringing pattern; there will be also the reverse interaction of the secondary pattern with the primary peak. For single objects the fringes are basically irrelevant, so that very close or identical radial velocities are determined using both techniques. Problems occur when multiple components are present in the spectra, and they are particularly severe in the CCF when the broadening of the lines is of the same scale as the line splitting, exactly the situation we face in our program.

We recognize that a method based on the two-dimensional cross-correlation function called TODCOR (Zucker & Mazeh 1994; Zucker et al. 1995) has been developed and successfully applied to several multilined stellar systems showing sharp spectral lines. We did not attempt to use this technique mostly because we feel more comfortable with a tool developed by ourselves, but also because (1) TODCOR is designed for sharp-line spectra and has not been demonstrated to work for the very broad lines of contact binaries,

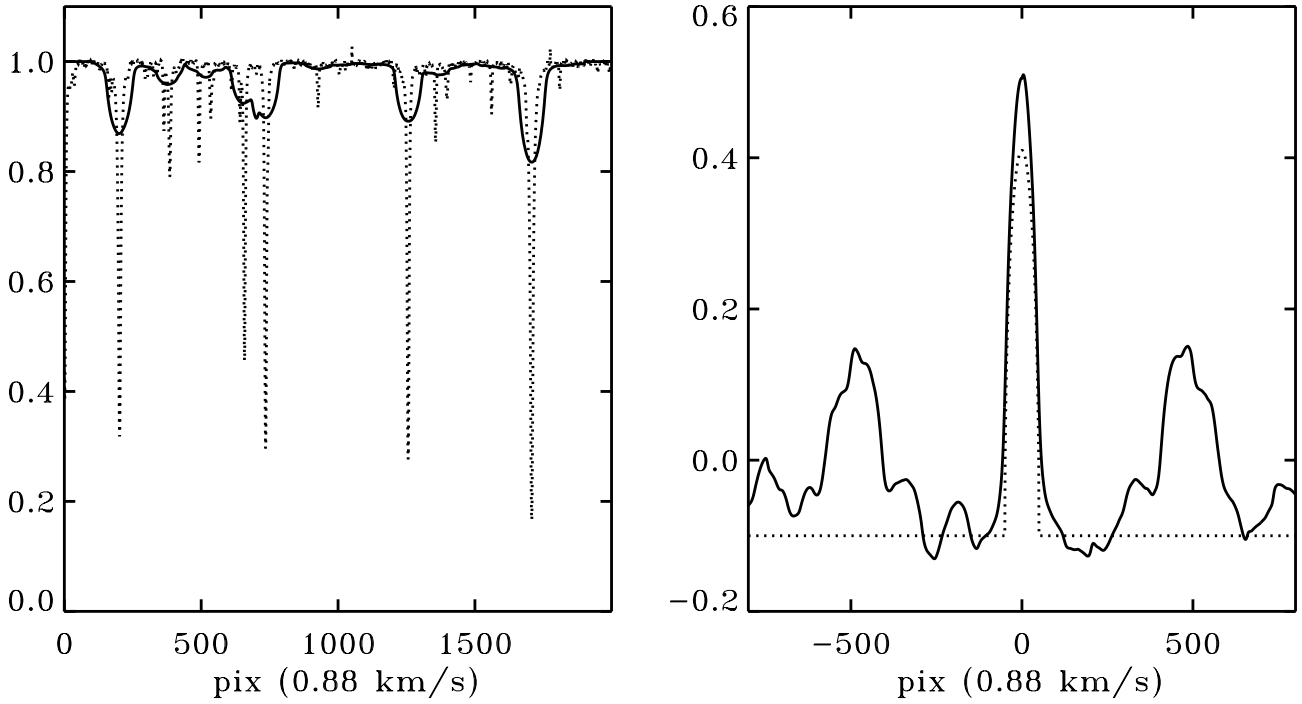

FIG. 2.—Experiment in data processing. *Left*: High-resolution spectrum rebinned to equal velocity steps of 0.88 km s^{-1}, without any additional broadening (*dotted line*) and with rotational broadening of $V \sin i = 88$ km s^{-1}. The CCF for the two spectra is shown in the right panel. Note the strong positive fringes outside the main correlation peak, as well as the shift of the quasi baseline well below the expected zero level; the actual broadening function has been shifted down by −0.1 units to visualize the most likely placement of the local baseline in the vicinity of the correlation peak.

and (2) we frequently deal with mixed very broad and narrow spectral signatures, which would require extension of the TODCOR capabilities even further. We note that the nonlinear nature of the cross-correlation complicates the derivation of the relative luminosities of components and requires a complex calibration, while our linear approach gives directly the relative luminosities through integration of the individual features in the broadening functions. This is particularly convenient for systems with components showing very different degrees of rotational broadening.

5. BROADENING FUNCTIONS

We define the broadening function[3] as a function that transforms a sharp-line spectrum of a standard star into a broadened spectrum of a binary, or for that matter of any other star showing geometrical, Doppler-effect line broadening. This way we not only determine the broadening-function shape but also automatically relate the absolute velocities of program stars to the radial velocity standards used as templates, a common advantage with the CCF approach. We do not use model spectra, e.g., through representation of spectral lines by delta functions. While the broadening functions determined that way would be cleaner and much better defined than those utilizing standard-star templates, the advantage of the automatic relative radial velocity calibration would be lost.

[3] A full description of the concept of the broadening functions with examples and detailed programming suggestions is available at http://www.astro.utoronto.ca/~rucinski.

We perform all radial velocity determinations in the geocentric system and only later transform the results to the barycentric (heliocentric with planetary corrections) system. Thus we start with a raw template spectrum $\boldsymbol{S}_t$, with its wavelength scale in $\boldsymbol{W}_t$, and a raw program spectrum $\boldsymbol{S}_p$, with its wavelength scale in $\boldsymbol{W}_p$. Both $\boldsymbol{S}_t$ and $\boldsymbol{S}_p$ are rectified and normalized to unity. To diminish the importance of the one-to-zero discontinuities at the ends of the spectra, we invert them so that the absorption lines are represented by positive spikes: $\boldsymbol{S}'_t = 1 - \boldsymbol{S}_t$ and $\boldsymbol{S}'_p = 1 - \boldsymbol{S}_p$.

The spectra must be of similar spectral type. We normally use the templates with spectra within one spectral type. However, we have found that F-type templates will work reasonably well for radial velocity determinations between middle A-types to early K-type stars; however, the relative luminosity estimates from the individual peaks will then be wrong.

The spectra must first be resampled into equal steps in velocity. In our case the velocity step is typically $\Delta v = 11.8$ km s^{-1}. An auxiliary vector of wavelengths is now created with elements $W_i = W_0(1 + r)^i$, where $i = 0, \ldots, n - 1$ is the index in the new vector and $r = \Delta v/c$, where c is the velocity of light. The origin of this vector, W_0, is selected to fall just above both origins of $\boldsymbol{W}_t$ and $\boldsymbol{W}_p$ for a meaningful interpolation of both spectra into the new wavelength scale. The length of $\boldsymbol{W}$ in our case is usually selected to be $n = 1000$–1020 spectral elements. The spectra $\boldsymbol{S}'_t$ and $\boldsymbol{S}'_p$ are linearly interpolated using $\boldsymbol{W}$, by treating $\boldsymbol{W}_t$ and $\boldsymbol{W}_p$ as the respective abscissae, to create the spectra used in the BF derivation: for the template T and for the program star P. After this is accomplished, the three wavelength vectors $\boldsymbol{W}$, $\boldsymbol{W}_t$, and $\boldsymbol{W}_p$ are no longer needed because the program and the template spectra are now in the same (geocentric) velocity

system. We can think about them as functions $P(n)$ and $T(n)$ with the same velocity axis or vectors $\boldsymbol{P}$ and $\boldsymbol{T}$ over the same range of indices.

The convolution operation, which maps a sharp-line spectrum T into a broad and/or binary-star spectrum P,

$$P(\lambda') = \int B(\lambda' - \lambda) T(\lambda) d\lambda \qquad (1)$$

can be written as an array operation

$$\boldsymbol{P} = \mathbf{D}\boldsymbol{B} , \qquad (2)$$

in which the rectangular array $\mathbf{D}$ is created from the vector $\boldsymbol{T}$ by placing it as columns of $\mathbf{D}$ after shifting it downward by one index for each successive column (see below or for further details consult Rucinski 1992, 1999). The broadening function is represented by a vector of the unknowns in the solution, $\boldsymbol{B}$. The array $\mathbf{D}$ has the short dimension m and the long dimension $n - m + 1$; it accomplishes the mapping of $T \rightarrow P$. We normally use the odd number for the size of the broadening function m to have it centered at the pixel symmetrically distant from both ends. Also, for proper handling of the ends, $m' = \text{integer}(m/2)$ points are removed from both ends of $\boldsymbol{P}$.

The convolution operation equivalent to equation (2), which is used in the least-squares determination of $\boldsymbol{B}$, can be written as a system of overdetermined linear equations:

$$P_i = \sum_{j=0}^{m-1} T_{i+m-j}\ B_j , \quad \text{with } i = m', \ldots, n - m' - 1 . \qquad (3)$$

The number of equations should be several times larger than the number of unknowns, $n - m + 1 > m$. In our program we normally use $n = 1000$–1020 and $m = 121$. The size of the broadening function m translates into the relative velocity range (program minus template) of ± 708 km s^{-1}, insuring a good definition of the BF itself and of the flat baseline around it. The actual size of the broadening function is a matter of choice; sometimes we repeat the BF determination with a smaller m for binary systems with moderate line splitting when a wide window of over 1400 km s^{-1} is not needed. The point is to use as short a BF as possible because the quality of the determination (overdeterminacy) increases in relation to how many times the spectra are longer than the BF.

Solving the broadening function B_j is accomplished by least squares. We are strong advocates of the singular value decomposition (SVD) technique, which is particularly useful in eliminating those parts of the spectra that carry no information (the interline continuum), but create linear dependencies. The approach involving rejection of small singular values is the best for restoration of the shape of the BF for its subsequent modeling. However, with the radial velocities in mind, we do not in fact eliminate any singular values. In this respect we have departed somewhat from the original philosophy, but this departure has a reason; if some basis functions are eliminated, there exists a possibility that the spectral features may acquire asymmetries through an unwanted conspiracy of the basis functions that remain in the definition of the BF. By retaining all singular values, we treat each element of B_j (eqs. [2]–[3]) as a totally independent variable not related in any way to its neighbors. Thus any least-squares technique can be used at this stage, although we continue to use the SVD because it is easier to use and more transparent for the matrix inversion.

The details of the SVD approach to solve the array equation, equation (2), or its equivalent, equation (3), for the BF vector $\boldsymbol{B}$ are described in Rucinski (1992), and the programming examples are given in Rucinski (1999). Even without elimination of any singular values in the SVD solution, this approach has an advantage that one decomposition of the template-spectrum array, $\mathbf{D} = \mathbf{U}\mathbf{W}\mathbf{V}^{\mathbf{T}}$, can serve to determine $\boldsymbol{B}$ from several program spectra through the inverted relation $\boldsymbol{B} = \mathbf{V}\mathbf{W}^{-1}(\mathbf{U}^{\mathbf{T}}\boldsymbol{P})$.

For an excellent exposition of the SVD technique stressing its beneficial properties, see Press et al. (1992).

Irrespective of which method of the least-square solution is used, the resulting broadening functions are always very noisy and cannot be used for radial velocity measurements. The reason for the excessive noise is that each element of the solution B_j is unrelated to its neighbors and is treated as a separate unknown. We know, however, that our spectral resolution is controlled by the spectrograph slit, which introduces coupling between neighboring points of the BF. In our case the intrinsic smoothing introduced by one of the entrance slits is characterized by the FWHM of about 2.6 or 2.2 pixels. It is therefore reasonable to apply some smoothing to the noisy BFs. Superficially, this step does the same to the final shape of the BF as smoothing through rejection of noise absorbed by high-order singular values in the SVD technique; however, this operation is strictly local, whereas the removal of some singular values may introduce nonlocal effects. Usually we smooth the broadening functions by convolving them with a Gaussian with $\sigma = 1.5$ pixels (FWHM = 3.53 pixels); for poor spectra of very faint stars we are sometimes forced to use $\sigma = 2.0$ (FWHM = 4.71 pixels). Such smoothing is slightly stronger than its instrumental counterpart by the spectrograph slit, but it is nevertheless very small when compared with widths of lines in binary stars with periods shorter than 1 day.

6. RADIAL VELOCITY MEASUREMENTS

Step 3 is the radial velocity determination from the broadening functions. We determine the radial velocities of each binary component in the geocentric system, relative to the template star, v_i. Following that, the relative velocities are transformed to the solar system barycenter with $V_i = v_i + (HC_p - HC_t) + V_t$, where HC are the barycentric (sometimes called "heliocentric") velocity corrections resulting from the orbital Earth motion for the program and template spectra and V_t is the barycentric velocity of the template star.

The broadening function $B(v)$ determined in the previous step is defined at points separated by equal steps in relative geocentric velocity, in our case normally $\Delta v = 11.8$ km s^{-1}, spanning the velocity range $-708 \leq V \leq +708$ km s^{-1}. The velocities of stellar components are determined by simultaneous fitting of several Gaussian curves to as many spectral features as are seen in the BF. Thus it would be a four-parameter Gaussian fit for a single star (baseline a_0, strength a_1, position a_2, width a_3), a seven-parameter fit for a binary or a 10-parameter fit for a triple system, etc., as in

$$B(v) \simeq a_0 + \sum_{i=1}^{n} a_{1i} \exp\left\{ -\left(\frac{v - a_{2i}}{a_{3i}} \right)^2 \right\} , \qquad (4)$$

where n represents the number of stellar components in the system. We found that least-squares Gaussian fits for single stars are usually stable, while those involving more components (binary, triple, and higher multiplicity systems) are numerically unstable, forcing us to fix or manually adjust the width parameters a_{3i}.

In the triple systems that we have encountered so far, the most typical combination has been a broad-lined close binary accompanied by a sharp-line, slowly rotating star. In such situations we first leave the width and position of the third, sharp component floating in order to determine the best possible parameters for its subsequent subtraction from the BF. For the example shown in Figure 1, the Gaussian widths for the binary components were *assumed* at $a_{31} = 110$ km s^{-1} and $a_{32} = 70$ km s^{-1}, while the width a_{33} was *determined* at 24.74 km s^{-1}. We found that situations similar to that shown in the figure require a careful removal of the third-component signature. In order to define the BF for the close binary the best way possible, we cannot remove the averaged signature of the third star from many spectra and must subtract it as it is defined for the same observation. There may be many reasons why subtraction of the averaged third-star peak leaves too large residuals, including small changes in the effective resolution, imperfections in the geocentric to barycentric transformations, or instabilities in the spectrograph. Obviously this approach reduces the accuracy of the third-star velocities, but our goal has been to determine the best velocities for the close binary, so we accept this limitation. The BF for the binary is usually very well defined; see for example Figure 4 in Paper IV for HT Vir.

The random radial velocity errors for binaries occurring in triple systems are only slightly larger than for the isolated binaries, typically by less than 1 km s^{-1} in the errors of V_0, K_1, and K_2; this increase may simply reflect more degrees of freedom in the problem (see the discussion in § 8, and Fig. 4). Much more difficult to characterize are systematic uncertainties. One manifestation of such uncertainties is the presence of an undesirable "cross-talk" in the three-feature fits in that the third-star velocities sometimes correlate with the binary phase. We always check the third-star velocities for dependence on the binary phase. We found such a correlation in three cases, SW Lyn in Paper IV and in V2388 Oph and II UMa in Paper VI; the rather extreme case of II UMa is explicitly discussed in Paper VI. It is usually quite difficult to find reasons for the cross-talk, and each case seems to be unique. Faintness of the star (SW Lyn) and/or poor spectra certainly magnify the problem, which appears to depend on such factors as the location of the third peak in the BF relative to the peaks for the binary system stars (i.e., with which component the third peak merges most of the time) or the overall degree of the line splitting for the binary system (which depends on the orbital inclination). Typically the cross-talk increases the error per observation of the third star from the expected level (for a sharp-line star) of 1.2–1.3 km s^{-1} to the level of 1.5–2.5 km s^{-1}. Except for noting the presence of the cross-talk, we are not in position to study it more extensively given the different type of the binary-phase dependence in each case. Our hope is that the cross-talk will average out in the velocities of the third component, although the final proof will come only through external comparisons. The stress has always been on the quality of the binary solutions, perhaps at the expense of the quality of the radial velocity data for the third components.

We measure the radial velocities for the binary components—and, if necessary, of a spectroscopic companion—but do not estimate the accuracy of the radial velocity measurements at this stage. In principle it is possible to establish a relation between the S/N in the spectrum and in the broadening function (Rucinski et al. 1993), but further propagation of the errors into the velocity errors is more complex and depends on many factors. While such a relation would definitely be needed for a full modeling of the BFs, we feel that the complexity of the error analysis is not warranted in our case. Thus we do not determine the radial velocity errors from the individual BFs but evaluate them externally later from the orbital velocity solutions. Such estimates may perhaps be overly pessimistic, as they incorporate systematic deviations from the orbital motion models. Most importantly, however, the random errors are not the limiting factor in our results; the real difficulty is in the evaluation of the systematic uncertainties. We address this issue in § 9 after describing the orbital solutions (§ 7) and the externally evaluated random errors (§ 8).

7. ORBITAL SOLUTIONS

Step 4 of the reductions is the determination of the radial velocity orbit using the individual velocities of both components at all observed orbital phases. Currently, we do so by measuring the individual velocities of components, although a more global approach involving the modeling of the broadening functions would definitely be much preferable. The broadening functions have the potential of providing much more information than just simple velocity centroids, so that the orbital solutions could be carried to a much higher level of sophistication than in this series of papers. Such use of the BFs was described in Rucinski (1992), Lu & Rucinski (1993), and Rucinski et al. (1993), where the modeling of the BF shape was advocated. Full modeling of this type requires knowledge of the orbital inclination, which is usually not available, and involves a simultaneous determination of the radial velocity span $K_1 + K_2$, the mass ratio q, and the degree-of-contact parameter f. The complexity of such a global approach is the main reason why we continue to use single velocities to characterize motions of stellar components, but we do recognize limitations of this approach, which may generate systematic uncertainties in the final results; this is discussed in § 9. We should add that originally this program was intended to provide the V_0-values from a small number of radial velocity measurements to relate to the then newly available *Hipparcos* tangential velocities. However, with time our program acquired its current significance as the main contributor of radial velocity orbits for short-period binaries (this circumstance taking place partly "by default" through a surprising lack of similar programs at other observatories). Thus we continue to use the Gaussian fits but recognize that all our spectra and the broadening functions may be used for a much more extensive modeling.

All short-period binary systems observed by us so far have circular orbits resulting in sine-curve variations of orbital velocities. The only exception that we had to consider is the third star in the system of HT Vir (Paper IV), which is on an eccentric orbit; for this case we used the model of Morbey (1975). Because eclipse effects of rotationally broadened lines change line shapes and produce undesirable radial velocity shifts, we eliminate observations close

to orbital conjunctions, usually within the phase ranges 0.85–0.15 and 0.35–0.65.

The orbital solutions are obtained iteratively. First, we use the linear model of two sine curves and one constant value, with an assumed moment of the primary eclipse T_0. Thus, for k observations, we simultaneously fit by least-squares $2 \times k$ equations of the type

$$V_1(\phi_l) = V_0 - K_1 \sin \phi_l + 0 \ , \quad (5)$$

$$V_2(\phi_l) = V_0 - 0 + K_2 \sin \phi_l \ ,$$

$$l = 0, \ldots, k-1 \ , \quad (6)$$

where ϕ is the orbital phase, $\phi_l = (t_l - T_0)/P$. Similarly to T_0, the period P is usually taken from literature sources and is fixed; only in a few cases we attempted to improve its value. The equations can be weighted at this point when observations are of different quality. The weighting schemes are discussed in descriptions of stellar systems in individual papers and are given in the tables with radial velocities. Note the sign convention in the equations, which implies that we usually start with an assumption that the primary, more massive component (star 1) is eclipsed at the photometric primary minimum. In other words we assume that, for a contact system, the configuration is of an A-type contact binary. We identify the W-type systems when this assumption is not valid.

The resulting V_0, K_1, K_2 are the first approximations of the orbital parameters. The next step in the iterative solution consists of the application of the linearized versions of equations (5)–(6) for ΔV_0, ΔK_1, ΔK_2, and ΔT_0. We always first use any available literature value for T_0 and then improve it by solving the linearized equations until all corrections Δ no longer change. It is at this stage that we determine random-error uncertainties of the orbital parameters and the radial velocity errors per observation.

8. MEAN STANDARD ERRORS

Least-squares solutions of the linearized equations (5)–(6) can provide the mean standard errors of the orbital parameters V_0, K_1, K_2, and T_0. We do not use such errors because they usually underestimate the random error uncertainties. Instead we use the "bootstrap-sampling" technique, which involves multiple (thousands of times) resampling of the data with possible repetitions, with subsequent solutions of all such data sets. By forming statistics of the spread in the resulting parameters and by determining the inner 67% distribution ranges, we estimate equivalents of the mean standard errors. They are sometimes close to the linear estimates but are usually larger. In any case we consider them to be more realistic as they include interparameter correlations.

We have a sufficient amount of information from all of our orbital solutions to analyze the sizes and distributions of our random errors. For that purpose we used all of the available solutions, eliminating three systems observed at the Dominion Astrophysical Observatory, as reported in Paper I, and adding W Crv, described separately (Rucinski & Lu 2000), totaling 58 orbital solutions altogether.

The statistics of the mean standard errors per single observation ϵ_i for the primary ($i = 1$) and the secondary ($i = 2$) components are shown in the top left panel of Figure 3. The median values of the errors are $\langle \epsilon_1 \rangle = 5.48$ km s^{-1} and $\langle \epsilon_2 \rangle = 11.50$ km s^{-1}. The corresponding distributions for the errors of the radial velocity amplitudes $\sigma(K_i)$ are shown in the top right panel. The median values are $\langle \sigma(K_1) \rangle = 1.11$ km s^{-1} and $\langle \sigma(K_2) \rangle = 1.96$ km s^{-1}. The center-of-mass velocities V_0 are better established than K_i because two stars contribute in each solution to one number. The median value of these errors is $\langle \sigma(V_0) \rangle = 1.07$ km s^{-1}. Finally, the distribution of the mean standard errors of the initial epoch $\sigma(T_0)$ is shown in the bottom right panel of Figure 3. The median value for this error is $\langle \sigma(T_0) \rangle = 0.0011$ days (about 1.5 minutes).

The mean standard errors of the orbital parameters are correlated. The most interesting correlations are shown in Figure 4. The two top panels show the mean error of the center-of-mass velocity $\sigma(V_0)$, which appears to be a convenient measure of the quality of the orbital data. It depends on the brightness of the system and on the orbital period. It is confined within less than 1.5 km s^{-1} for $V_{\max} < 8.5$ but increases to slightly over 2 km s^{-1} for $V_{\max} \geq 10$ (*top left*). The scatter in $\sigma(V_0)$ increases for short-period systems (*top right*), but this may be due to the fact that most of our targets had periods within 0.3–0.6 days, in a range where a genuine frequency maximum exists in the volume-limited samples of contact binaries (Rucinski 1998). The systems with longer periods ($P > 0.8$ days) tend to show small errors, but these are exactly the binaries that had been overlooked before among the bright stars and have been easy targets for our program. The error $\sigma(V_0)$ correlates tightly with $\sigma(K_i)$ and with ϵ_i, as shown in the four bottom panels of Figure 4. A particularly close correlation with the slope close to unity exists between $\sigma(K_1)$ and $\sigma(V_0)$ (*middle left*).

Binaries observed in spectroscopic triple systems show slightly larger random errors than when isolated, typically by less than 1 km s^{-1} in the errors of V_0, K_1, and K_2. Such binaries are shown by open symbols in all plots in Figure 4.

9. SYSTEMATIC UNCERTAINTIES

It is difficult to evaluate systematic uncertainties of our results. The systematic errors depend in a complex way on the orbital parameters and couple with the random errors. The main source of systematic errors is the measurement of radial velocities from the broadening functions. We approximate the center-of-mass positions with the light centroids and measure the centroids by fitting Gaussians. The latter assumption, that the radial velocities of the light centroids coincide with radial velocities of the mass centers, is—in general—not fulfilled by distorted components in close binary systems and is particularly dangerous for contact binaries where the peaks in the BFs are not symmetric, with steeper outer parts and more gently sloping inner parts. Direct modeling of the BFs would avoid this systematic error (see the end of this section).

Some insight into systematic uncertainties involving the Gaussian approximation of the peaks in the broadening functions can be obtained by applying Gaussians of various widths and evaluating systematic shifts in the results. We will consider here, as a case study, a typical, 9 mag, A-type contact system, GM Dra, from the immediately preceding paper in this series, Paper VI.

Let us first consider one broadening function for the orbital phase 0.283 of GM Dra (*bottom*, Fig. 5). For this particular broadening function we would normally select

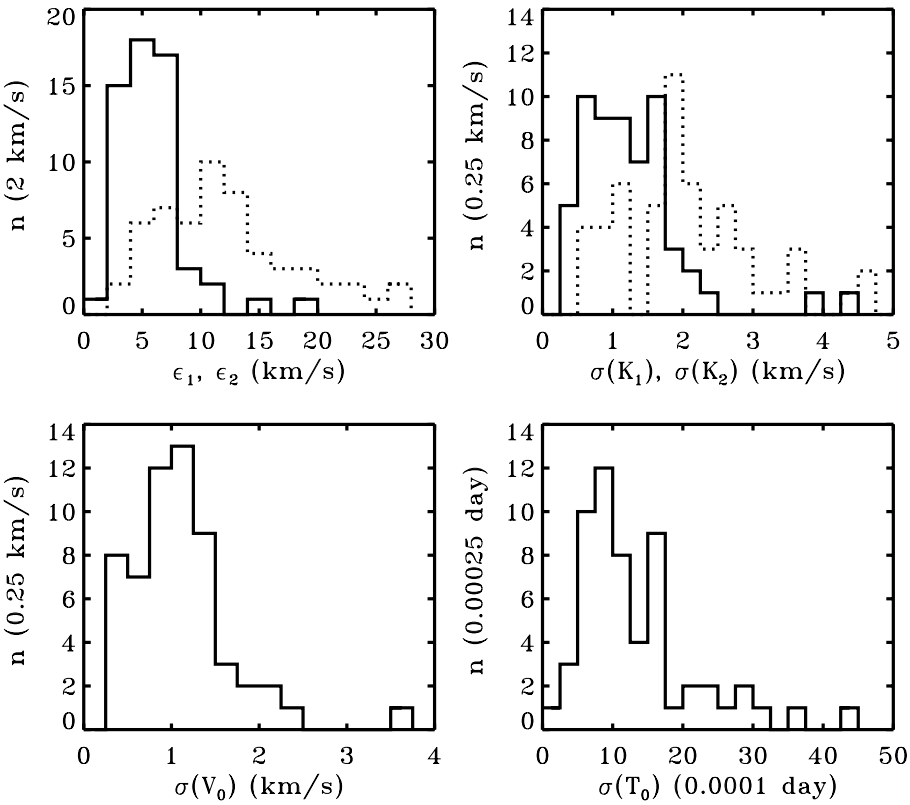

FIG. 3.—Distributions of mean standard errors for program binaries. The histograms give the distributions of the error per observation (for each component) ϵ_i and of the errors of orbital parameters $\sigma(V_0)$, $\sigma(K_1)$, and $\sigma(K_2)$, all expressed in kilometers per second. The bin sizes are given in the y-axis labels. In the two top panels solid-line histograms are for the primary components [ϵ_1 and $\sigma(K_1)$], while the dotted histograms are for the secondary components [ϵ_2 and $\sigma(K_2)$]. The last panel gives the distributions of mean standard errors for the initial epoch T_0 in units of 0.0001 days.

the best-fitting Gaussians to have the width parameters $a_{31} = 120$ km s^{-1} and $a_{32} = 80$ km s^{-1} (see eq. [4]). However, as an experiment, we considered widths between the estimated narrowest and widest acceptable values of a_{3i}: $a_{31} = 100$–140 km s^{-1} and $a_{32} = 60$–100 km s^{-1}. The extreme cases are shown by dotted and broken lines in Figure 5. For the full range of widths the change in the measured velocity of the primary component is from -28.86 km s^{-1} to -31.27 km s^{-1}, while the change for the secondary component is from $+261.44$ km s^{-1} to $+262.49$ km s^{-1}. Thus systematic errors in radial velocities appear to be at a level of 1.5 to 2.5 km s^{-1}, with larger velocities (in the absolute sense) associated with larger assumed widths of the fitting Gaussians.

Analysis of the type presented above can be done for all available broadening functions at all orbital phases. The four top panels of Figure 5 show the shifts in the measured centroids for all available observations of GM Dra, obtained around the orbital quadratures within the orbital phase ranges 0.15–0.35 and 0.65–0.85, as marked in the figure. The Gaussian widths a_{3i} were incremented in equal steps, and for each assumed width a full radial velocity determination was performed. As we can see in the figure, the systematic effects are clearly present, especially for the secondary (less massive) component. The shifts are typically at the level below 2 km s^{-1} for the primary component, but shifts of the order 5–7 km s^{-1} are not uncommon for the secondary component. The shifts depend on the side of the binary system (or the sign of the radial velocity) observed at a given orbital quadrature. The overall tendency appears to be that the wider Gaussian width a_{3i} results in velocities farther away from the center-of-mass velocity, i.e., ones that should lead to systematically larger values of the orbital amplitudes K_i. This is confirmed by the actual determinations of the radial velocity orbits for the extreme values of (a_{31}, a_{32}) pairs, selected to deviate from the optimal values of 120 and 80 km s^{-1} by ± 20 km s^{-1}. The systematic changes for the particular case of GM Dra strongly depend on the parameter considered. While the changes in V_0 are within $+0.09$ and -0.16 km s^{-1}, those in the amplitudes are larger: -0.34 and $+0.15$ km s^{-1} for K_1 and as much as -4.30 and $+5.97$ km s^{-1} for K_2. While the ranges of the Gaussian widths a_{3i} were intentionally exaggerated in the experiment to estimate the largest systematic deviations, we clearly see that systematic effects may set an important limitation on our results. For comparison, we note that the random errors of the orbital parameters of GM Dra are $\sigma(V_0) = 1.52$ km s^{-1}, $\sigma(K_1) = 1.75$ km s^{-1} and $\sigma(K_2) = 2.50$ km s^{-1} (Paper VI). Thus, for this particular binary, the systematic uncertainty appears to be larger than the random error only for K_2, but then it is even 2 times larger.

Optimally, the systematic effects resulting from the use of different widths in the Gaussian fits should be evaluated for each binary through a process similar to that applied to GM Dra. However, we feel that it is impractical to perform similar analyses for all systems in this program. Besides we know that the application of the Gaussian fits is—in any case—a crude approximation and that the best approach would be

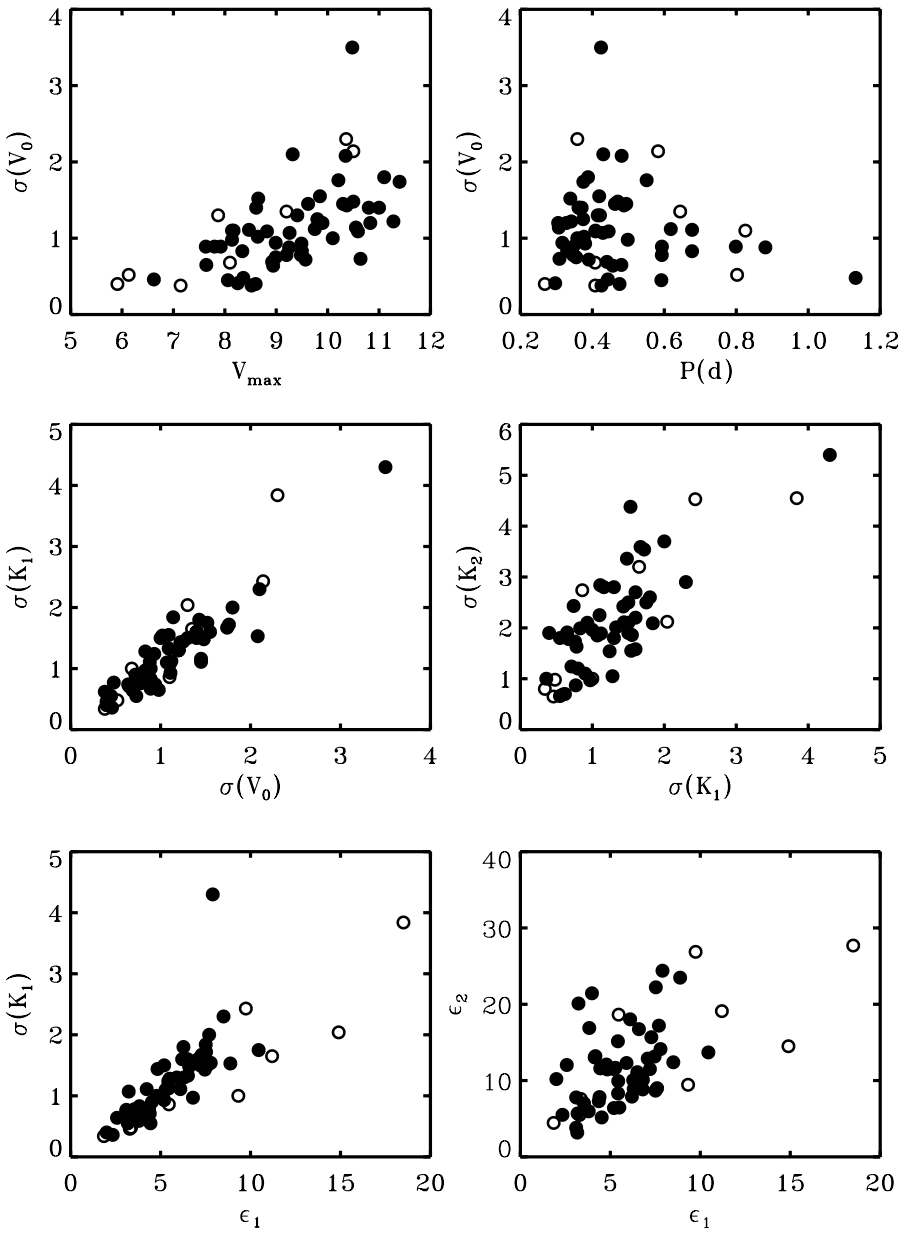

FIG. 4.—Correlations between various mean standard errors as given in the axis labels. *Top*: $\sigma(V_0)$ as a function of V_{max} and the orbital period, P. $\sigma(V_0)$ is a convenient measure of the solution quality and correlates tightly with $\sigma(K_1)$, as shown in the middle left panel. The middle right panel shows the correlation between $\sigma(K_1)$ and $\sigma(K_2)$. This correlation is not perfect because of the very large range of mass ratios observed among binaries of this program. The two bottom panels show the errors per observation ϵ; the left panel shows the correlation between ϵ_1 and $\sigma(K_1)$, while the right panel shows the correlation between ϵ_1 and ϵ_2. In all panels binaries analyzed through subtraction of the third-component signatures from the broadening functions are marked by open circles. All quantities are expressed in kilometers per second.

to *model* the broadening functions as was done in Rucinski (1992), Lu & Rucinski (1993), and Rucinski et al. (1993). Full BF modeling would permit the inclusion of more spectra than we utilize now, because currently we measure for radial velocities only those BFs which show a clear splitting of the spectral signatures. By the addition of these spectra we would increase the available material by about 20%–30%, which would only slightly reduce random errors and thus produce a very modest improvement in accuracy. Much more important would be a reduction or the entire elimination of the systematic errors, which may reach levels of 5–7 km s^{-1}. For most binaries in this program, this would typically correspond to about 2%–3% error in K_i, but in some extreme cases of small semiamplitudes, the errors may reach 10%–15%. While the approach involving combined radial velocity and light-curve modeling would avoid the main systematic effects, it would require a considerable organizational and computational effort, introducing large delays in our mostly observational program. Since our radial velocity observations are—for most systems—the first and the only ones, we decided to accept the level of systematic errors generated by the use of the measuring Gaussians and make our solutions generally available, keeping in mind their systematic uncertainties, which must be taken into account when considering the overall accuracy of our program.

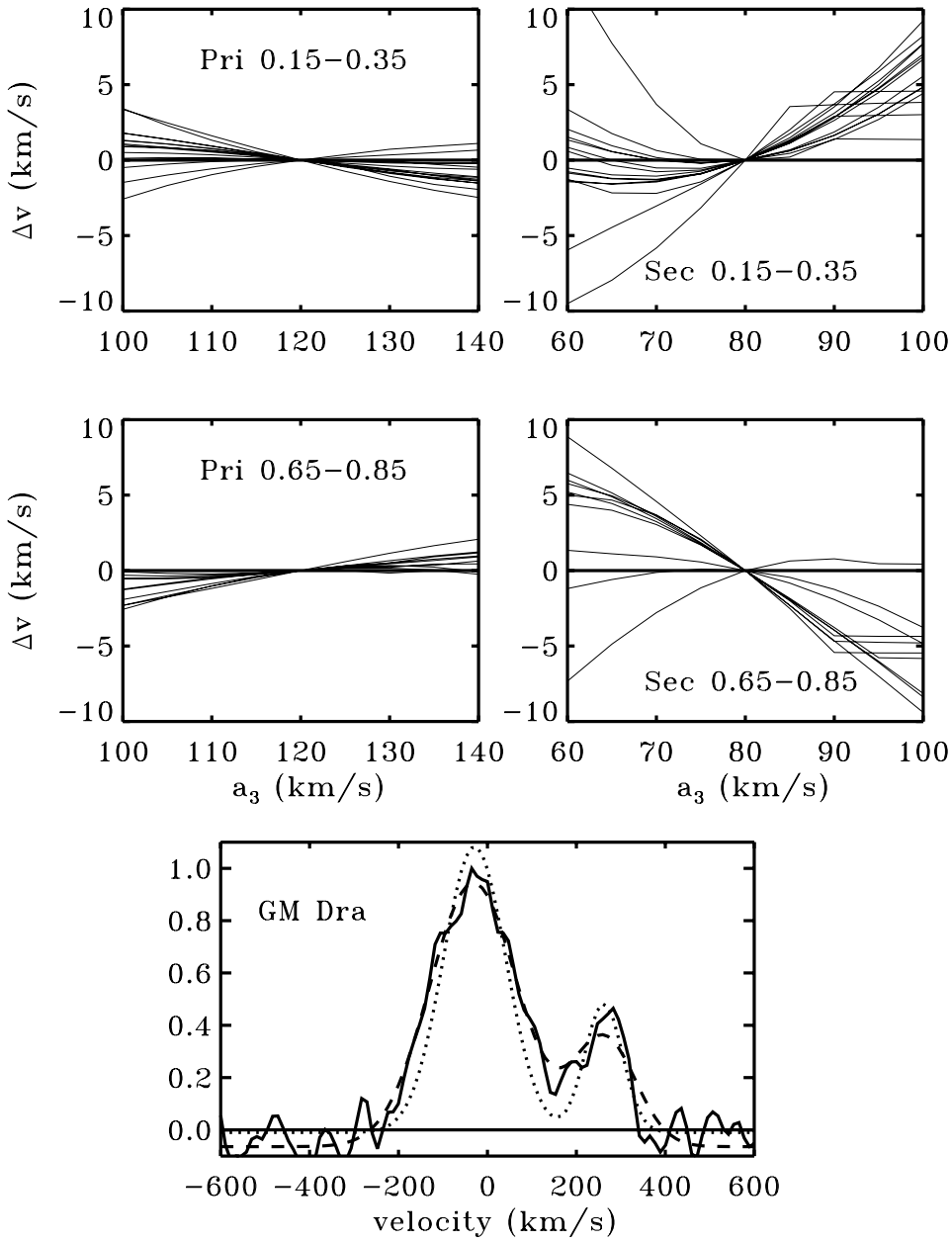

FIG. 5.—*Top four panels*: Shifts in the measured velocities for the primary (*left*) and secondary (*right*) components of GM Dra (Paper VI) vs. the Gaussian-width parameter a_{3i} (see text). Each line is for one broadening function at one orbital phase within ranges around the two orbital quadratures, as marked in the panels. The bottom panel shows one broadening function of GM Dra at the orbital phase 0.283, approximated by the Gaussians with the width parameters [a_{31}, a_{32}] considered most extreme for this case: (100, 60) km s^{-1} (*dotted line*) and (140, 100) km s^{-1} (*broken line*).

10. CONCLUSIONS AND PLANS

The ongoing survey of close binary systems with periods shorter than 1 day currently being conducted at the David Dunlap Observatory has resulted in a consistent set of radial velocity orbits for 60 previously unobserved binaries to approximately the 11th magnitude. While at the start the survey concentrated on systems that simply had not been studied before (for various reasons, but mostly because of inadequate instrumentation and data-analysis tools some half a century ago, when this field was very active), the photometric discoveries of the *Hipparcos* satellite are now dominating in numbers. There was only one *Hipparcos* system among the first 20 orbits (Papers I and II), nine such systems among the next 20 orbits (Papers III and IV) and 15 such systems among the most recent 20 orbits (Papers V and VI). About 50 known, photometrically discovered binaries still remain to be observed and analyzed, and new ones are constantly added to catalogs, some of them quite bright. Regrettably, apparently there is no similar survey for the southern hemisphere.

Our survey is quasi-random in the sense that we observe all short-period ($P < 1$ day), bright, previously unobserved binaries. With such criteria the contact binaries absolutely dominate in numbers. Among the 60 systems described in the previous six papers, only eight were not contact systems. This is partially due to strong selection effects against the detection of detached binaries, but mostly due to the very

high frequency of contact binary systems in the old-disk population, particularly in the period range 0.3 to 0.5 days but with a tail extending beyond 1 day, to about 1.3–1.5 days. The high frequency of incidence is strongly manifested in the volume-limited OGLE sample and in open clusters (Rucinski 1998). Because our survey is magnitude limited, we tend to include many brighter systems from the tail of the distribution between 0.5 days and our current upper limit of 1 day. Otherwise, we do not discriminate among binary systems in any other way. In particular, the random character of the survey has resulted in discoveries of the largest ($q = 0.97$, V753 Mon; Paper III) and the smallest ($q = 0.066$, SX Crv; Paper V) known mass ratios among contact binaries.

The DDO survey is characterized by moderate random errors of about 1–2 km s^{-1} for the orbital parameters V_0, K_1, and K_2, and—upon completion—can serve as a useful database of parameters of very close binary systems. We are aware, however, that our final parameters contain systematic uncertainties resulting from our radial velocity measurement techniques. While the use of the broadening functions permitted us to analyze close binaries in several multiple, visual/spectroscopic systems, providing data which were too " difficult " before, our extraction of individual radial velocities from the broadening functions through Gaussian fitting is a disputable approach for contact binary systems. Because the line broadening for such systems is very strong, comparable to orbital velocities of hundreds of kilometers per second, and—in fact—somewhat asymmetric, our measuring technique may lead to systematic errors reaching levels of 5–7 km s^{-1} or even more. Paradoxically, through the use of the broadening functions in place of the cross-correlation functions, we have uncovered real physical reasons why the Gaussian approximation is only barely appropriate. The correct approach avoiding the systematic errors would be to model the broadening functions and determine the radial velocities in terms of the mass ratio q and the scaling factor $(K_1 + K_2)$, with the shift V_0. The models would require independent input from parallel solution of light curves, providing the orbital inclination angle i as well as the degree of contact f. Currently, most of the program targets have not had their light curves solved, and, even if some attempts have been made, we would not trust them for the following simple reason: we have seen so many cases of the spectroscopic mass ratio being different from the previous photometric mass-ratio determinations, $q_{\rm sp} \neq q_{\rm phot}$, that we feel very strongly that the values of $q_{\rm phot}$ are usually not properly constrained and may be plainly wrong[4]. But then the chances of total eclipses depend on the mass ratio itself (a wider range of inclinations for small values of q), producing a very complex bias in the uncertainties of $q_{\rm phot}$, leading to entirely incorrect combinations of orbital parameters.

We envisage that the results of this survey will provide just a first stage of an iterative process. In the future, our spectroscopic values of the mass ratio $q_{\rm sp}$ should permit the solution of light curves that were previously unsolvable because of the poorly constrained mass ratios. The derived information on (i, f) pairs would permit, in turn, a rediscussion of the broadening functions and determination of the final orbital parameters free of systematic uncertainties.

Concerning the instrumental developments at the DDO, soon we plan to start using a new CCD system based on a much more sensitive detector. While the analysis of the data should remain the same as described above, we may have to select the targets more discriminately. In particular, it may turn out to be impractical to observe all binaries with periods shorter than 1 day down to the expected limiting magnitude of about 12.5 mag. Indeed, from the point of astrophysical usefulness, it would be advantageous to reduce the deficit of the intrinsically faint contact systems among spectroscopically studied binaries of the magnitude-limited sample by attempting to form a volume-limited sample by giving preference to very short-period systems.

While many persons have participated in this program and have either coauthored the previous papers or their contributions have been acknowledged there, special thanks are due to Dr. Hilmar Duerbeck, who contributed to setting the goals of the program in its early stages when it was concerned mostly with the center-of-mass velocities for contact binaries for a planned spatial-velocity investigation. The author would like to thank Stefan Mochnacki and Mel Blake for reading and commenting on an early version of the paper. Thanks are also due to the anonymous referee for three very careful and constructive reviews, which will certainly contribute to the improvement of this series of the papers.

Support from the Natural Sciences and Engineering Council of Canada is acknowledged with gratitude.

[4] Totally eclipsing systems are an exception, as pointed out by Mochnacki & Doughty (1972a, 1972b).

REFERENCES

Evans, N. R. 2000, AJ, 119, 3050
Lu, W., & Rucinski, S. M. 1993, AJ, 106, 361
———. 1999, AJ, 118, 515 (Paper I)
Lu, W., Rucinski, S. M., & Ogloza, W. 2001, AJ, 122, 402 (Paper IV)
Mochnacki, S. W., & Doughty, N. A. 1972a, MNRAS, 156, 51
———. 1972b, MNRAS, 156, 243
Morbey, C. 1975, PASP, 87, 689
Press, W. H., Teukolsky, S. A. Vetterling, W. T., & Flannery, B. P. 1992, Numerical Recipes in FORTRAN (2d ed.; Cambridge: Cambridge Univ. Press)
Rucinski, S. M. 1992, AJ, 104, 1968
———. 1998, AJ, 116, 2998
———. 1999, in ASP Conf. Ser. 185, Precise Stellar Radial Velocities, ed. J. B. Hearnshaw & C. D. Scarfe (San Francisco: ASP), 82
Rucinski, S. M., & Lu, W. 1999, AJ, 118, 2451 (Paper II)
Rucinski, S. M., & Lu, W. 2000, MNRAS, 315, 587
Rucinski, S. M., Lu, W., Capobianco, C. C., Mochnacki, S. W., & Blake, M. 2001, AJ, 122, 1974 (Paper V)
Rucinski, S. M., Lu, W., Capobianco, C. C., Mochnacki, S. W., Blake, R. M., Thomson, J. R., Ogloza, W., & Stachowski, G. 2002, AJ, 124, 1738 (Paper VI)
Rucinski, S. M., Lu, W., & Mochnacki, S. W. 2000, AJ, 120, 1133 (Paper III)
Rucinski, S. M., Lu, W., & Shi, J. 1993, AJ, 106, 1174
Stefanik, R. P., Latham, D. W., & Torres, G. 1999, in ASP Conf. Ser. 185, Precise Stellar Radial Velocities, ed. J. B. Hearnshaw & C. D. Scarfe (San Francisco: ASP), 354
Sugars, B. J. A., & Evans, N. R. 1994, JRASC, 88, 270
Zucker, S., & Mazeh, T. 1994, ApJ, 420, 806
Zucker, S., Torres, G., & Mazeh, T. 1995, ApJ, 452, 863